

EFFECTIVE VOID RATIO AND RACK LENGTH DEFINITION BY EXPERIMENTAL MEASUREMENTS OF FLOW WITH GRAVEL SIZE SEDIMENT THROUGH BOTTOM RACKS

LUIS G. CASTILLO⁽¹⁾, JUAN T. GARCÍA⁽²⁾ & JOSÉ M. CARRILLO⁽³⁾

⁽¹⁾ Dept. of Civil Engineering, Universidad Politécnica de Cartagena, Spain,
e-mail luis.castillo@upct.es

⁽²⁾ Dept. of Civil Engineering, Universidad Politécnica de Cartagena, Spain,
e-mail juan.gbermejo@upct.es

⁽³⁾ Dept. of Civil Engineering, Universidad Politécnica de Cartagena, Spain,
e-mail jose.carrillo@upct.es

ABSTRACT

This work is focused on the study of bottom rack intake systems located in ephemeral and torrential streams. Clear water, and water with gravel sediments have been analyzed. Different tests have been carried out to quantify the influence of the solids passing through the racks. The wetted rack lengths and the efficiency of racks are studied. The clear water has been also modeled with computational fluid dynamics, and compared with the measured obtained at Universidad Politécnica de Cartagena. Experimental and numerical studies that characterize both, the clear water and the influence of solid load in the operation of the bottom racks, will allow us to improve the existing design criteria.

Keywords: Bottom intake systems, racks, gravels, CFD.

1. INTRODUCTION

Bottom rack intake systems are used to collect the maximum quantity of water on small, steeply sloping mountain rivers with important sediments transport. Due to the fact that the bed load sediment transport passes over the racks, they have to operate under extreme conditions (Bouvard, 1992).

Most design recommendations try to avoid the rack occlusion. Some of them are based on prototype measurements. The main parameters are:

- The bar clearance, that must be higher than the biggest grain sizes transported during floods.
- The longitudinal rack slope. The increase in the rack slope tends to reduce the probability of sediment load over it.
- The percentage of increment in the opening area of the rack by the consideration of the surface partially clogging.
- The construction of an upstream stilling basin, that regulates the size of the incoming sediments.

Based on intake systems located in the French Alps, Ract-Madoux et al. (1955) proposed a bar clearance near 0.100 m and a longitudinal rack slope near 20%. Using Tyrolean weirs of Tiroler Kraftwerke AG, Simmler (1978) and Drobir (1981), recommend to use a bar clearance around 0.150 m, with $d_{95} \approx 0.060$ m, a longitudinal rack slope between 20 and 30%, and a rack opening area increment factor from 1.5 to 2.0. Based on the same bottom intakes systems that Ract-Madoux et al., Bouvard (1992) considered a bar clearance close to 0.100-0.120 m (0.020-0.030 m in case of intake systems for power plants), an slope of racks between 30 and 60%, and area of rack opening factor from 1.5 to 2.0. Raudkivi (1993) recommended a minimum bar clearance of 0.005 m for a longitudinal rack slope near 20%. The shape of the bars has been also analyzed to know the amount of derived flow (Orth et al., 1954; Frank, 1956; Nosedá, 1956; Drobir, 1981, 1999; Bouvard, 1992).

Actually, experimental and numerical studies are focused on the analysis of solids passing over bottom racks. Ahmad and Kumar (2010) studied in laboratory the percentage of solids passing through the rack. The authors considered the longitudinal rack slope, different water flows, and the ratio between the size of sediments and the bar clearance (from 0.18 to 0.83). Castillo et al. (2013a, b, c) carried out numerical simulations with computational fluid dynamics (CFD) methodology. They analyzed the increment in the wetted rack length due to the sediment transport. Different sediment concentrations (from 1.0 to 5.0% in volume), void ratios from 0.16 to 0.60, flow rates and rack slopes. Castillo et al. (2014) analyzed the influence of gravels whose d_{50} value was close to the spacing between bars. Different longitudinal rack slopes, water flows and solids concentrations were used. Tests showed a reduction of the collected flow due to the occlusion of the rack. The reduction seems to be related with the longitudinal rack slope. The maximum efficiency was obtained with a slope of 30%.

In the analysis of clear water flows, some simplifications are often assumed: the flux over the rack is one-dimensional, the flow decreases progressively, the hydrostatic pressure distribution acts over the rack in the flow direction, the energy level or energy head is considered constant along the rack.

Several researchers analyzed these simplifications by means of laboratory hydraulic models. Nosedá (1956) studied the clear water flow through different racks. The author defined a expression to calculate the discharge coefficient, valid for horizontal rack case and subcritical approximation flow:

$$C_q = 0.66m^{-0.16} \left(\frac{h}{l} \right)^{-0.13} \quad [1]$$

where l is referred the distance between the centerline of two consecutive bars, m the void ratio, and h the height of water measured in the vertical direction.

According to Brunella et al. (2003), the differences between measured and calculated water depth profiles are generally found at the beginning of the rack, and at the end of the rack when wall friction effects are neglected. Differences at the beginning of the rack are due to the consideration of hydrostatic pressure distribution.

Righetti and Lanzoni (2008) calculated the flow collected by the rack with the following differential equation:

$$dq(x) = C_q m \sqrt{2g(H_0 + \Delta z)} dx \quad [2]$$

where m is the void ratio, dx the differential rack length in the flow direction, H_0 the total energy at the beginning of the rack, Δz the vertical distance between the edge of the rack and the analyzed section, and C_q the discharge coefficient. The same authors considered that $C_q \approx \sin \alpha$, being α the angle between the velocity vector of water collected by the rack and the plane of the rack.

Several researchers proposed expressions to calculate the wetted rack length L required to collect a determined flow (Table 1).

Table 1. Formulations for flow profiles and wetted rack lengths.

Author	Formulation	Parameters
Bouvard and Kuntzmann (1954)	$L = \left\{ \frac{1}{2m''} \left[\left(j + \frac{1}{2j^2} \right) \arcsin \sqrt{\frac{j}{j + (1/2j^2)}} + 3\sqrt{\frac{1}{2j}} \right] + \left(\frac{0.303}{m''^2} + \frac{2j^3 - 3j^2 + 1}{4j^2} \right) \right\} \cdot h_1 \cdot \cos \varphi$ $j = \frac{h_1}{h_c}; \quad m'' = m \cdot C_q$	h_1 = depth at the beginning of the rack; h_c = critical depth; m'' = product of the void ratio and the discharge coefficient
Nosedá (1956)	$L = \frac{E_0}{C_q \cdot m} [\Phi(y_2) - \Phi(y_1)]; \quad \Phi = f(y); \quad y = \frac{h}{E}$ $L = 1.1848 \frac{E_0}{C_q \cdot m}$ $\Phi = \frac{1}{2} \arccos \sqrt{y} - \frac{3}{2} \sqrt{y(1-y)}$	E_0 = specific energy at the beginning of the rack;
Frank (1956)	$L = 2.561 \frac{q_1}{\lambda \sqrt{h_1}}; \quad \lambda = m C_{q0} \cdot \sqrt{2 \cdot g \cdot \cos \varphi}; \quad C_{q0} = 1.22 C_{q, x=x_0}$	h_1 = depth at the beginning of the rack; q_1 = incoming specific flow φ = angle of the rack with the horizontal plane
Krochin (1978)	$L = \left[\frac{0.313 q_1}{(C_q k)^{3/2}} \right]^{2/3}; \quad k = (1-f)m; \quad f = 0.15 - 0.30$ $C_q = C_0 - 0.325 \tan \alpha$ $C_0 = 0.6 \text{ if } m \geq 4$ $C_0 = 0.5 \text{ if } m < 4$	q_1 = incoming specific flow; f = obstruction coefficient

2. MATERIALS AND METHODS

2.1 Physical device

An intake system has been constructed in the Hydraulic Laboratory of the Universidad Politécnica de Cartagena. It consists of a 5.00 m long and 0.50 m wide approximation channel, a rack with different slopes (from horizontal to 33%), a discharge channel and the channel to collect derived water. Figure 1 shows the water thought the rack when gravels are tested.

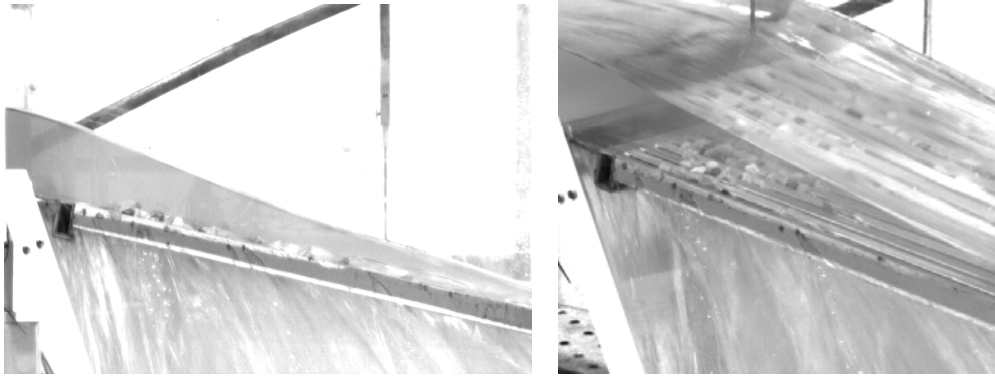


Figure 1. Gravel test in the laboratory device at the Hydraulic Laboratory of Universidad Politécnica de Cartagena.

Test with clear water have been done by using the three racks (A, B, and C) with 0.9 m lengths. All of them are made of aluminum bars with T profiles (T 30/25/2 mm). Bars are disposed longitudinally to the inlet flow. The difference between the racks is the spacing between bars, so different void ratios are available. Table 3 summarizes the geometric characteristics of each rack.

Table 2. Geometric characteristic of the tested racks.

	A	B	C
Spacing between bars (mm)	5.70	8.50	11.70
Void ratio $m = \frac{b_1}{b_1 + 30}$	0.16	0.22	0.28

Different specific flows (53.8, 77.0, 114.6, 138.88, and 155.4 l/s/m), and rack slopes (0%, 10%, 20%, 30%, 33%) have been considered. The inlet flow, q_1 , is measured in an electromagnetic flowmeter at the beginning of the channel. The rejected flow, q_2 , is measured by using a V-notch weir located in the channel that collects the rejected flow. The flow derived by the rack, q_d , is calculated as a difference between q_1 and q_2 . In each test, the flow depth along the rack and the wetted rack length were measured.

To test the hydraulic behavior of the intake system, the laboratory measurements were used to model and calibrate computational fluid dynamics (CFD) simulations. CFD codes solve the differential Reynolds-Averaged Navier-Stokes (RANS) equations of the phenomenon in the fluid domain, retaining the reference quantity in the three directions for each control volume identified. The equations for conservation of mass and momentum may be written as:

$$\frac{\partial \rho}{\partial t} + \frac{\partial}{\partial x_j} (\rho U_j) = 0 \quad [3]$$

$$\frac{\partial \rho U_i}{\partial t} + \frac{\partial}{\partial x_j} (\rho U_i U_j) = -\frac{\partial p}{\partial x_i} + \frac{\partial}{\partial x_j} (2\mu S_{ij} - \overline{\rho u_i u_j}) \quad [4]$$

where i and j are indices, x_i represents the coordinate directions ($i = 1$ to 3 for x , y , z directions, respectively), ρ the flow density, t the time, U the velocity vector, p the pressure, u_i' presents the turbulent velocity in each direction ($i = 1$ to 3 for x , y , z directions, respectively), μ is the molecular viscosity, S_{ij} is the mean strain-rate tensor, and $-\overline{\rho u_i u_j}$ is the Reynolds stress. Eddy-viscosity turbulence models consider that such turbulence consists of small eddies which are continuously forming and dissipating, and in which the Reynolds stresses are assumed to be proportional to mean velocity gradients. The Reynolds stresses may be related to the mean velocity gradients and eddy viscosity by the gradient diffusion hypothesis:

$$-\overline{\rho u_i u_j} = \mu_t \left(\frac{\partial U_i}{\partial x_j} + \frac{\partial U_j}{\partial x_i} \right) - \frac{2}{3} \delta_{ij} \left(\rho k + \mu_t \frac{\partial U_k}{\partial x_k} \right) \quad [5]$$

with μ_t being the eddy viscosity or turbulent viscosity, $k = 1/2 \overline{u_i u_i}$ the turbulent kinetic energy and δ the Kronecker delta function.

The CFD volume finite scheme program ANSYS CFX (version 14.0) has been used. The k - ω based Shear-stress-Transport (SST) turbulence model was selected to complement the numerical solution of the Reynolds-averaged Navier-Stokes equations (RANS). To solve the two-phase air-water, the homogeneous model was used. The fluid domain is divided into control volumes, which must satisfy the balance of the governing equations. The total number of elements used in the

simulations was around 350,000 elements, with 0.004 m length scale near the rack. For simplicity, it has been considered that all the longitudinal bars work in the same mode in the intake system. For this reason, the domain fluid considers three bars and two spacing between bars. Symmetry conditions were used in the central plane of the extreme bars.

The model boundary conditions correspond to the flow at the inlet condition (located 0.50 m upstream of the rack), the upstream and downstream water levels and their hydrostatic pressures distributions. In the bottom of the water collected channel, opening boundary condition were used. It has been assumed that the free surface is on the 0.5 air volume fraction. Figure 2 shows the velocity vectors in the rack C ($m = 0.28$), with 30% slope and $q_1 = 138.88$ l/s/m.

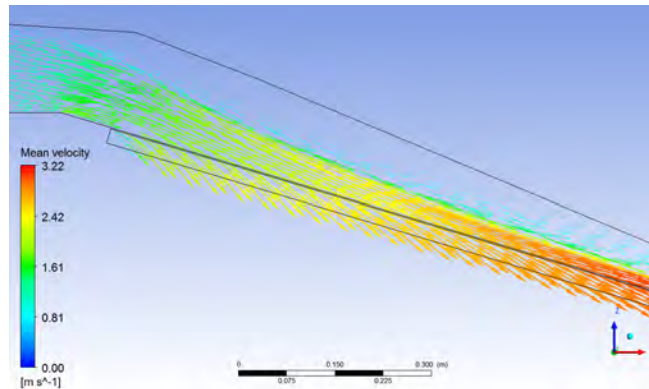


Figure 2. Velocity vectors calculated with numerical simulations for rack C, $q_1 = 138.88$ l/s/m, and 30% slope.

3. RESULTS AND DISCUSSION

3.1 Clear water experimental tests

We have compared the angle of the velocity vector of water, measured in the centre of the spacing between bars with the horizontal plane. Righetti et al. (2000) obtained in their lab studies range of this angle between 25 and 35 degrees, reducing according the depth water decrease. The sinus of this angle may be used to estimate the discharge coefficient of the water collected through the rack. Figure 3 shows the results obtained with numerical simulations using CFD programs for the specific flow $q_1 = 155.4$ l/s/m and different slopes when the rack C ($m = 0.28$) is tested. The angle tends to increase with the slope of the rack. Although the model is not the same than the used by Righetti et al. (2000), the values obtained are in the same rate than the observed in lab, reducing the angle with the decreasing of the depth water over the rack.

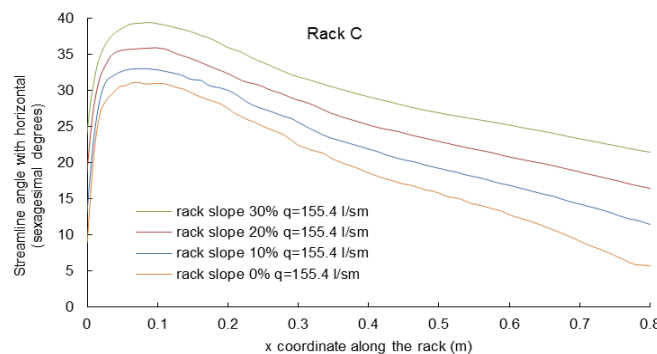


Figure 3. Angle of velocity vector with horizontal in the plane of the rack.

3.2 Sediment experimental tests

For evaluate the effect of the sediment transport over the rack, two gravel-size materials have been analyzed. The sieve curves are almost uniform. The average grain size is $d_{50} = 8.3$ mm for gravel 1 and $d_{50} = 14.8$ mm for gravel 2. Castillo et al. (2014) compared the results obtained in clear water and in water with gravel transport.

In this study, racks B (void fraction $m = 0.22$) and C ($m = 0.28$) were used to test the gravel transport. In rack B, tests were carried out by using gravel 1, using three specific flows ($q_1 = 77.0, 114.6$ and 155.4 l/s/m), and five slopes ($i = 0, 10, 20, 30$ and 33%). In rack C, gravel 2 was used, considering three specific flows ($q_1 = 114.6, 138.88$ and 155.4 l/s/m), and the same five slopes.

Sediments are uniformly added at the beginning of the inlet channel. The inlet point of the sediments is located 5 meters upstream of the rack. The solid flow at the beginning of the channel was $q_s = 0.33$ kg/s. Hence, solid concentrations in volume at the inlet of the channel were between 0.16 and 0.34%, depending on the water flow tested.

Each condition was repeated twice. Tests were continued until that all the solids reached the downstream side of the rack. The duration of the test was between 700 and 1620 seconds.

In the tests, the flows derived by occluded racks have been measured. To define effective void ratio in occluded racks, m' , a differential equation of constant energy head is numerically solved using the fourth-order Runge–Kutta algorithm. The system of equations is equivalent to the solution of two ordinary differential equations for $h(x)$ and $q(x)$. At the inlet section, two boundary conditions are considered: the inlet specific flow q_1 and the initial energy E_0 (estimated as the critical energy head). The discharge coefficient value is obtained with equation [1] (Noseda, 1956). The numerical computation interval for x is 0.05 m. The numerical results for $h(x)$ are successfully compared with clear water test data. The energy equation to obtain m' is

$$\frac{dh}{dx} = \frac{m'0.66m'^{-0.16}\left(\frac{h}{l}\right)^{-0.13} 2\sqrt{h \cos \alpha (E_0 - h \cos \alpha)}}{3h \cos \alpha - 2(E_0)} \quad [6]$$

$$\frac{dq}{dx} = -C_q m \sqrt{2gh \cos \alpha} \quad [7]$$

where α is the angle of longitudinal rack with horizontal.

The effective void ratio, m' , is obtained for a rack length of 0.9 m in agreement with the laboratory model. An effective discharge coefficient, C_q' , may be obtained considering that the rack maintains its initial void ratio, m :

$$C_q' = \frac{m'}{m} \left[0.66m'^{-0.16} \left(\frac{h}{l} \right)^{-0.13} \right] \quad [8]$$

Figures 4 and 5 show the effective void ratio, m' , and the effective discharge coefficient, C_q' , for the rack B with gravel 1 and the rack C with gravel 2, respectively, and results compared with clear water values. The m' and the C_q' values are much bigger when the experiment is carried out with clear water. With sediments, they tend to increase with the increase of the inlet flow and the slope of the rack. The maximum values are obtained for racks with slopes of 30 and/or 33%, while the increment of the inlet flows seems to reach a constant value for both parameters for inlet flows bigger than 114.6 l/s/m in rack B and 138.88 l/s/m in rack C.

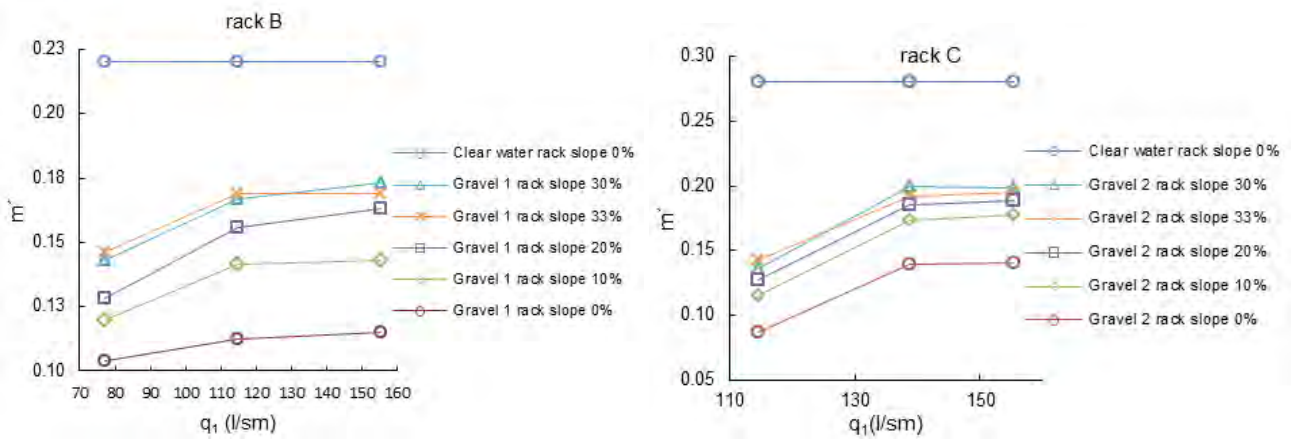


Figure 4. Effective void ratio values m' for different inlet flow rates and racks B and C, respectively.

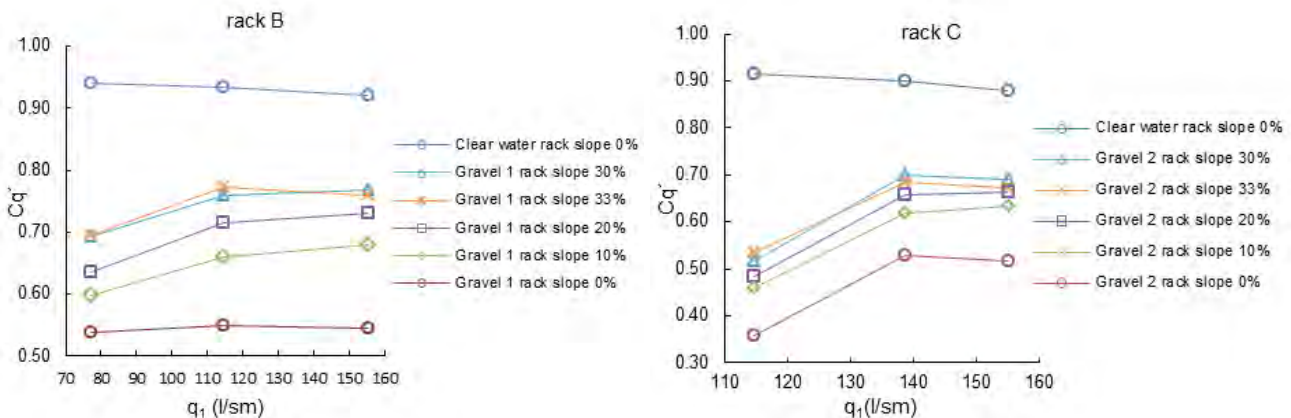


Figure 5. Effective discharge coefficient values C_q' for different inlet flow rates and racks B and C, respectively.

From these effective void ratios, m' , equation [6] has been reevaluated to calculate the total wetted rack length necessary to collect the total inflow, q_1 . Figures 6 and 7 show the wetted rack length calculated for different q_1 and rack slopes. Data are compared with the wetted lengths calculated by Nosedá (1956), Frank (1956), Bouvard and Kuntzmann (1956) and Krochin (1978) in horizontal racks. Krochin values consider an obstruction percentage $f = 30\%$. The results obtained by Krochin are closer to the laboratory results than the obtained with the formulas proposed by the other authors.

Wetted rack lengths with effective void ratios are longer than those measured with clear water: This is due to the gravel occlusion of the bar clearance. The occlusion is more important with the decrease of the rack slope (Figures 6 and 7). Others parameters to take into account are the inlet flow rate and the gravel size. The reduction in the inlet flow q_1 , drives to smaller wetted rack lengths.

We can see that for the rack B ($m = 0.22$), slope 30% and specific flow rate $q_1=114.6$ l/s/m, the required rack length increases from 0.93 m, calculated with the Nosedá formula (valid in clear water and horizontal racks), to 1.15 m when gravel occlusion is considered. The wetted rack length has increased near 24% of the initial required rack length. For the rack C ($m = 0.28$), slope of 30% and $q_1 = 138.88$, the rack length increases near 29% of the initial required rack length.

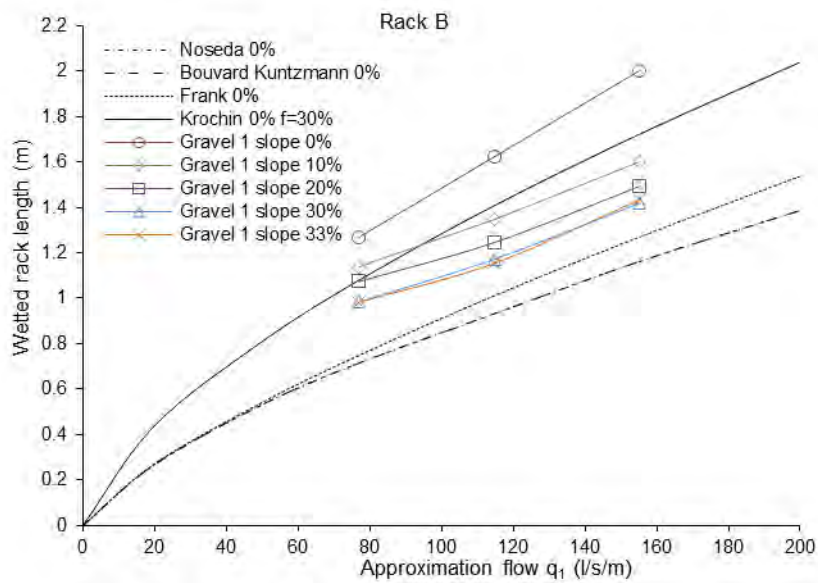


Figure 6. Wetted rack length of rack B calculated for each inlet flow rate and for different rack slopes.

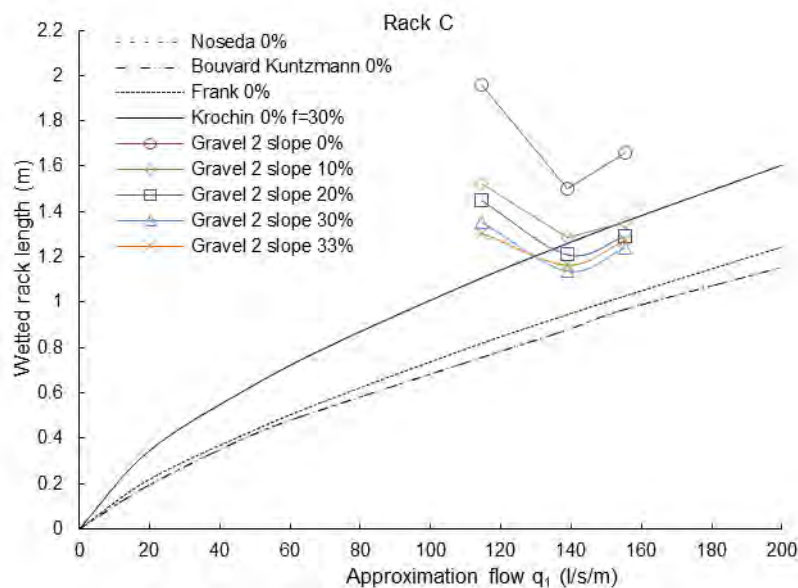


Figure 7. Wetted rack length of rack C calculated for each inlet flow rate and for different rack slopes.

In general, the deposition of the gravels drives to a growth of the required wetted rack length in comparison with clear water flows. With the specific flows considered in the rack B (Figure 6), gravels tend to sweep to the downstream side due to the fact that the push over them is bigger than the forces that limit their movement. In the rack C (Figure 7), the smaller specific flows tested do not generate enough forces to sweep the gravels. Hence, the occlusion area increases and the required wetter rack length is bigger. With higher inlet flows, the gravels tend to sweep to the downstream side.

The deposition of the gravels in the spacing between bars is not homogeneous. Preferential occlusion zones are observed in the places where the angle of the streamlines with the rack plane is higher. In Figure 8 we can see the zones of deposition of gravels for the same flow rate ($q_1=155.4$ l/s/m) and two different rack slopes (0 and 30%).

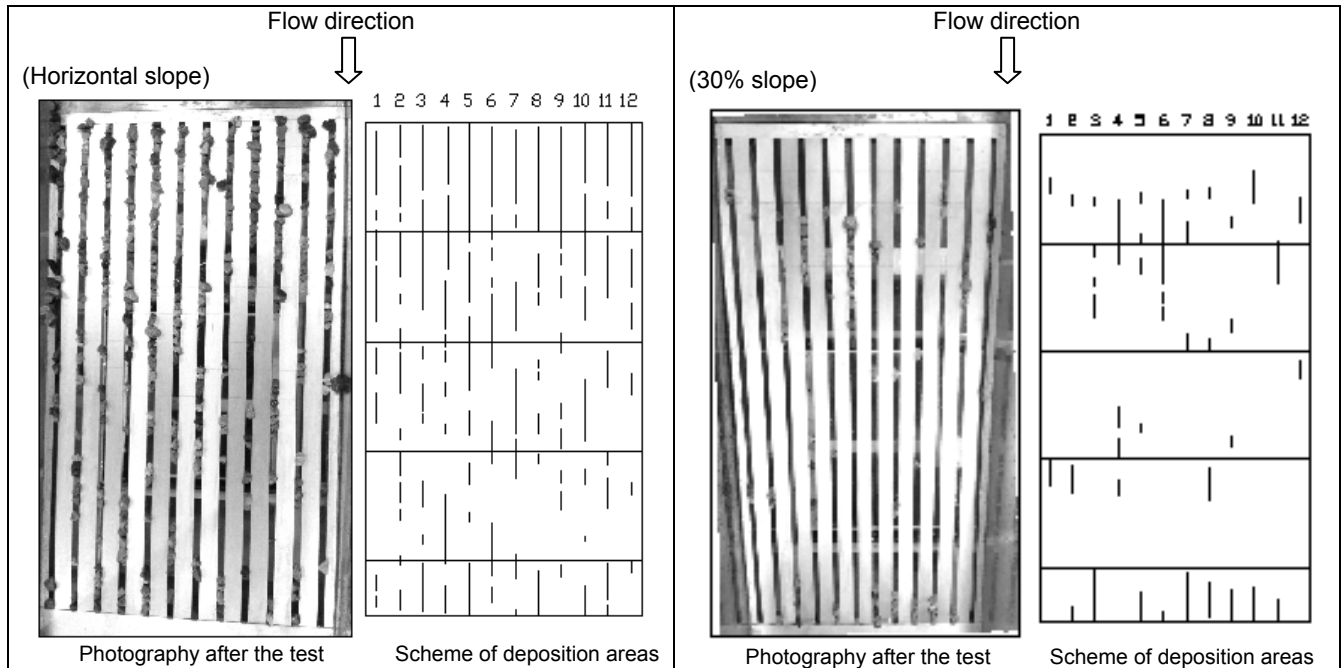


Figure 19. Occlusion of bar clearance for $q_1 = 155.4$ l/s/m and slopes of 0 and 30%, respectively.

At the beginning of the rack is observed a non deposition area due to the initial fall distance of the gravels. This distance tends to increase with the rack slope. There is a stagnation zone at the end of the rack due to the spacing between bars disappears. That leads to a local deposition of gravels. For the rack with slope horizontal, the main deposition zone is observed from the beginning of the rack until near 0.60 m. For the rack slope 30%, the main deposition area is from 0.10 to 0.15 m. Later we can find small deposition areas along the rack .

The equilibrium forces due to the drag and weight over the gravels deposited in the spacing clearance may be expressed by the following equation

$$W \sin \alpha + C_d \rho \left(\frac{V_b^2}{2} \right) A \cos(\Phi - \alpha) \geq \text{tg} \varphi \left(W \cos \alpha + C_d \rho \left(\frac{V_b^2}{2} \right) A \sin(\Phi - \alpha) \right) \quad [9]$$

where W is the weight of the gravel deposited in the spacing, α the angle of the rack with the horizontal plane, C_d the drag coefficient, ρ the density of clear water, V_b the magnitude of the velocity vector, A the projection of the particle in a plane perpendicular to the velocity vector, Φ the angle of the velocity vector with the horizontal, and φ the particle friction angle.

In this experiments, the Reynolds number is near 4000, the shape of the deposited gravels is rod, with a ratio $a/c \approx 2$, being a , b and c the length in the major, transverse and minor axis, being a oriented in the main flow direction (Zingg, 1935). In these conditions the drag coefficient may be adopted as $C_d = 0.60$ for the gravel 2 (Sotelo, 2004).

Equation [9] has been solved by considering the gravel 2 ($a = 0.038$ m, $b = 0.020$ m and $c = 0.015$ m). Hence, the particle friction angle has been obtained along the rack with a value close to 54° .

4. CONCLUSIONS

In this work, bottom intake systems have been analyzed in order to utilize them in ephemeral rivers. Due to that in semiarid regions the rain episodes are torrential, the objective is to derivate the maximum water with the minimum amount of sediment. The shape and spacing between bars are parameters that need to be considered as a function of sediment transport that occurs in the river. Design criteria of bottom rack intake systems in mountain rivers usually considers a bar clearance higher than d_{90} . This study enables to know the behavior of bottom systems in case of a reduced bar clearance from the point of view of the occlusion.

Clear water simulations solved with CFD code have obtained a good agreement with experimental data, when several flows and rack slopes where considered.

Effective void ratios, and rack lengths are defined by experimental measurements of flow with gravels, taking into account the occlusion effect. A potential equation relating the shear stress at the beginning of the rack with the effective void ratio has been proposed. This allows to calculate the increment of wetted rack length in gravels with d_{50} near or superior to the

spacing between bars. In general, wetted rack lengths considering occlusion are in agreement with the formulae proposed by Krochin (1978) when an obstruction coefficient of 30% is considered.

Preferential deposition zones along the rack are observed in laboratory. The friction angle between gravels and the rack may be calculated by equilibrium of forces. This allows us to estimate the clogged zones as a function of the solids characteristics.

More experimental tests should be done considering diverse sieve curves, rack with different void ratios, slopes, and shape of bars. To find the occlusion percentage, field studies are required to know the liquid and solid flows that reach in the intake system.

REFERENCES

- Ahmad, Z., and Kumar S., (2010). Estimation of trapped sediment load into a trench weir, 11th International Symposium on River Sedimentation (ISRS), University of Stellenbosch, South Africa, Sept. 6-9, 2010, pp.1-9.
- ANSYS, Inc. (2010). ANSYS CFX-Solver Theory Guide. Release 13.0.
- Bouvard, M. (1953). Debit d'une grille par en dessous. *La Houille Blanche* 2: 290-291
- Bouvard, M., and Kuntzmann, J. (1954). Étude théorique des grilles de prises d'eau du type "En dessous". *La Houille Blanche* 5: 569-574
- Bouvard, M. (1992). Mobile Barrages & Intakes on Sediment Transporting Rivers. IAHR Monograph. Rotterdam: Balkema.
- Brunella, S., Hager, W., and Minor, H. (2003). Hydraulics of Bottom Rack Intake. *Journal of Hydraulic Engineering*, 129(1): 2-10.
- Castillo, L.G., and Lima, P. (2010). Análisis del dimensionamiento de la longitud de reja en una captación de fondo. Proc. XXIV Congreso Latinoamericano de Hidráulica, Punta del Este, Uruguay, 21-25 November 2010.
- Castillo, L., and Carrillo, J.M. (2012). Numerical simulation and validation of intake systems with CFD methodology. Proc. 2nd IAHR European Congress; Munich, 27-29 June 2012.
- Castillo, L.G., Carrillo, J.M., and García, J.T. (2013a). Comparison of clear water flow and sediment flow through bottom racks using some lab measurements and CFD methodology. Proc. Seven River Basin Management. Wessex Institute of Technology; New Forest, 22-24 May 2013.
- Castillo, L.G., Carrillo, J.M., and García, J.T. (2013b). Flow and sediment transport through bottom racks. CFD application and verification with experimental measurements. Proc. 35th IAHR Congress, Chengdu, 8-13 September 2013.
- Castillo, L.G., Carrillo, J.M., and García, J.T. (2013c). Comparativa del flujo de agua limpia y con sedimentos a través de sistemas de captación de fondo utilizando datos de laboratorio y un modelo CFD. Proc. III Jornadas de Ingeniería del Agua, Valencia, 23-24 October 2013
- Castillo, L.G., García, J.T., and Carrillo, J.M. (2014). Experimental measurements of flow and sediment transport through bottom racks. Influence of graves sizes on the rack. Proc. International Conference on Fluvial Hydraulics (RIVER FLOW), Lausanne, Switzerland, 3-5 september 2014
- Drobir, H. (1981). Entwurf von Wasserfassungen im Hochgebirge. In, *Österreichische Wasserwirtschaft*: 11(12): 243-253.
- Drobir, H., Kienberger, V. & Krouzecky, N. (1999). The wetted rack length of the Tyrolean weir. Proc. 28th IAHR Congress, Graz, 22-27 August 1999.
- Frank, J. 1959. Fortschritte in der hydraulik des Sohlenrechens. *Der Bauingenieur*, 34: 12-18.
- Frank, J. 1956. Hydraulische Untersuchungen für das Tiroler Wehr. *Der Bauingenieur*, 31(3): 96-101
- Krochin, S. 1978. *Diseño Hidráulico*. Segunda Edición. Colección Escuela Politécnica Nacional. Quito, Ecuador.
- Noseda, G. 1956. Correnti permanenti con portata progressivamente decrescente, defluenti su griglie di fondo. *L'Energia Elettrica*, 565-581.
- Orth, J., Chardonnet, E. & Meynardi, G. (1954). Étude de grilles pour prises d'eau du type. *La Houille Blanche* 3: 343-351.
- Ract-Madoux, M., Bouvard, M., Molbert, J., and Zumstein, J. 1955. Quelques réalisations récentes de prises en-dessous à haute altitude en Savoie. *La Houille Blanche*, 6: 852-878.
- Raudkivi, A.J. (1993). *Hydraulic Structures Design Manual*. IAHR, pp – 92-105.
- Righetti, M., Rigon, R., and Lanzoni, S. 2000. Indagine sperimentale del deflusso attraverso una griglia di fondo a barre longitudinali. Proc. XXVII Convegno di Idraulica e Costruzioni Idrauliche, Genova, 3: 112–119.
- Righetti, M., and Lanzoni, S. 2008. Experimental Study of the Flow Field over Bottom Intake Racks. *Journal of Hydraulic Engineering* 134(1): 15-22.
- Simmler, H. (1978). *Konstruktiver Wasserbau*. Technische Universität Graz. Institut für Wasserwirtschaft und konstruktiven Wasserbau.
- Sotelo, G. (1997). *Hidráulica General*. Volumen I. Fundamentos. Limusa Noriega Editores, México D.F.
- Zingg, T. 1935. Beitrag Zur Schotteranalyse, Schweiz. Mineralog. und Petrog. Mitt.,Bd., 15: 39-140, 1935.